Perturbation of Adsorbed CO by Amine Derivatives Coadsorbed on the γ-Al_2O_3 Surface: FTIR and First Principles Studies

Sunhee Kim,[†] Dan C. Sorescu,[‡] Oleg Byl,[†] and John T. Yates, Jr.*[,†]

Surface Science Center, Department of Chemistry, University of Pittsburgh, Pittsburgh, Pennsylvania 15260, and U.S. Department of Energy, National Energy Technology Laboratory, Pittsburgh, Pennsylvania 15236

Received: October 27, 2005; In Final Form: January 9, 2006

The coadsorption of CO and triethylenediamine (TEDA) (also called 1,4-diazabicyclo[2.2.2]octane, DABCO) on a high-area γ-Al_2O_3 surface has been investigated with use of transmission FTIR spectroscopy. It has been found that TEDA binds more strongly to both Lewis acid sites and to Brønsted Al−OH sites than does CO. Competition experiments indicate that TEDA displaces CO to less strong binding sites. Evidence for weak CO···TEDA interactions is found in which small ν(CO) redshifts are produced. Comparison between different amines such as triethylenemonoamine (TEMA) (also called 1-azabicyclo[2.2.2]octane, ABCO), trimethylamine (TMA), and ammonia indicates that the ν(CO) redshift increases with increasing amine polarizability, indicating that the redshift is mainly due to dipole image damping effects on the CO oscillator frequency. The direct bonding between the exposed N lone pair electrons of the TEDA molecule and CO does not occur. First principles theoretical studies have characterized the bonding of CO with γ-Al_2O_3 Lewis acid sites of various types as well as TEDA bonding to both Lewis acid sites and to Al-OH groups. The theoretical studies also indicate that strong bonding of adsorbed CO with TEDA molecules does not occur, and that the observed decrease in the binding energy of CO when coadsorbed with TEDA on γ-Al_2O_3 is expected.

Introduction

The adsorption behavior of triethylenediamine (TEDA) (also called 1,4-diazabicyclo[2.2.2]octane, DABCO) on the high-area γ-Al_2O_3 surface has been studied previously with transmission FTIR spectroscopy.[1−3] It was demonstrated that TEDA binds to Al−OH Brønsted acid sites via hydrogen bonding as well as to Al^{3+} Lewis acid sites on the Al_2O_3 surface. TEDA adsorption by hydrogen bonding involves the formation of both Al−OH···(TEDA) and Al−OH···$(TEDA)_2$ species.

Since TEDA has been used to enhance the adsorption capacity of various high-area surfaces (charcoal, silicate, zeolite, etc.) for capture of chemical agents,[4−8] we have investigated the role of TEDA functionalization of γ-Al_2O_3 on the adsorption of carbon monoxide, using transmission FTIR spectroscopy. We find that CO binds weakly to TEDA on the Al_2O_3 surface causing the CO vibrational mode to be redshifted by -8 cm^{-1} from the frequency of CO(g). For this study other amines such as triethylenemonoamine (TEMA) (also called 1-azabicyclo-[2.2.2]octane, ABCO), trimethylamine (TMA), and ammonia have also been employed for comparison with TEDA functionalization of γ-Al_2O_3 surfaces.

II. Experimental and Computational Methods

A. Experiment. The experimental methods used in this work are described in detail in ref 2. The turbo-pumped ultrahigh vacuum system (base pressure $<1 \times 10^{-8}$ Torr) is designed to study a high area solid surface by transmission IR spectroscopy. A tungsten grid, into which γ-aluminum oxide powder is pressed at 70 000 psi, is clamped to a manipulator assembly with copper mounting rods which serve to conduct electrical heating current to the sample as well as to cool the sample using contact with liquid N_2 held in a reentrant Dewar insert in the IR cell. A thermocouple is welded to the grid to measure and control the temperature of the sample between 83 and 1500 K.

The Al_2O_3 powder is obtained from Guild Associates (surface area = 250 m^2/g, which was measured before heat treatment). The prepared Al_2O_3 sample is heated to 1000 K for 1 min in a vacuum to produce a highly dehydroxylated surface.[2,9−13] Triethylenediamine (TEDA) and triethylenemonoamine (TEMA) are obtained from Aldrich and used without further purification. Trimethylamine (TMA) and ammonia were also employed. Gases are introduced into the chamber quantitatively and the gas line is evacuated with a sorption pump and a turbo-molecular pump between the dosages of different gases.

The infrared spectra are recorded with a Bruker TENSOR 27 FT-IR spectrometer. Each spectrum is obtained by averaging 128 interferograms with 2 cm^{-1} resolution and the background spectrum taken through the empty grid region is subtracted.

B. Computational Method. Two sets of calculations have been performed in the current study. The first set aimed to describe gas-phase properties and the interaction between TEDA and CO molecules in the gas phase. These investigations have been done with the Gaussian 03 suite of programs.[14] In this case the geometrical structure optimizations and vibrational frequency calculations have been done at the MP2/cc-pVDZ theory level. Further analysis of polarizability for a small set of amines (NH_3, TMA, TEMA, and TEDA) has been performed at the MP2/cc-pVDZ level. In the case of NH_3 and TMA and TEDA molecules the polarizability results have been further refined by calculations at the MP2/aug-cc-pVTZ level.

The second set of theoretical investigations focused on description of the interaction between TEDA and CO molecules

* Address correspondence to this author.
[†] University of Pittsburgh.
[‡] National Energy Technology Laboratory.

10.1021/jp056183z CCC: $33.50
Published on Web 02/22/2006

upon adsorption on the γ-Al_2O_3 surface. The calculations performed in this study were done with the Vienna ab initio simulation package (VASP).[15−17] This program evaluates the total energy of periodically repeating geometries based on density-functional theory and the pseudopotential approximation. In this case the electron−ion interaction has been described by fully nonlocal optimized ultrasoft pseudopotentials (USPPs) similar to those introduced by Vanderbilt.[18,19] Periodic boundary conditions are used, with the one-electron pseudo-orbitals expanded over a plane-wave basis set. The cutoff energy used in these calculations was 495 eV corresponding to precision level *high* in VASP code.[20]

All calculations related to adsorption properties of CO and TEDA molecules on the γ-Al_2O_3 surface have been done with the PW91 generalized gradient approximation (GGA) of Perdew et al.[21] The sampling of the Brillouin zone was performed by using a Monkhorst−Pack scheme,[22] using grid mesh with a k-point separation of 0.05 $Å^{-1}$. The minimization of the electronic free energy was performed by using an efficient iterative matrix-diagonalization routine based on a sequential band-by-band residuum minimization method (RMM)[16,17] or alternatively based on preconditioned band-by-band conjugate-gradient (CG) minimization.[23] The optimization of different atomic configurations was performed by conjugate-gradient minimization of the total energy.

The crystallographic structure of bulk γ-alumina was taken according to that reported in ref 24. In this model the monoclinic crystallographic unit cell of γ-Al_2O_3 contains 8 Al_2O_3 formula units. On the basis of a fit of the dependence of the unit cell energy on the corresponding cell volume with the Murnaghan equation of state,[25] an optimum volume of the unit cell of 381.592 $Å^3$ has been determined. The calculated cell volume per Al_2O_3 unit of 47.69 $Å^3/Al_2O_3$ unit is about 2.82% larger than the one obtained experimentally (46.39 $Å^3/Al_2O_3$ unit).[26] The bulk modulus at zero pressure obtained from a Murnaghan analysis is 166.7 GPa, a value that is also close to the reported experimental data of 162 ±14 GPa.[27] The corresponding optimized lattice parameters were found to be a_{calcd} = 5.598 Å, b_{calcd} = 8.432 Å, c_{calcd} = 8.083 Å, and β = 90.53°. These values are slightly larger by about 1.5% than those reported previously by Digne et al. based on plane-wave calculations with a cutoff energy of 300 eV.[24] As was shown in previous studies[24,28,29] the predominant surface orientations of γ-alumina are the (110) surface (70−83%) followed by the (100) surface, which accounts for about 17% of the exposed surface. Consequently, in the current study we focused on these two types of surfaces exclusively. Following ref 24 these surfaces have been simulated by using slab models with at least eight atomic planes (see Figure 1). Each slab was taken to be symmetrical to avoid unphysical dipole−dipole interactions between neighbor slabs. For the (110) and (100) surfaces the calculated surface energies were found to be 1498 and 958 mJ/m^2, similar to values of 1540 and 970 mJ/m^2, respectively, obtained by Digne et al.[24] Following notation introduced in ref 24 the (100) surface presents 5-fold coordinated aluminum atoms (denoted as Al_V) and 3-fold coordinated oxygen atoms (denoted as μ_3-O in Figure 1a). In contradistinction, the (110) surface (see Figure 1b) presents several types of coordinated Al and O atoms, namely 3-fold Al_{III} (I) and 4-fold Al_{IV} (II and III) aluminum sites and 2-fold μ_2-O and 3-fold μ_3-O oxygen atoms.

Besides the description of surface properties, the plane-wave DFT method employed in the current work is also adequate for description of molecular systems of interest, namely CO and TEDA molecules. For example, the optimized bond length of an isolated CO molecule was found equal to 1.1453 Å and the vibrational frequency ν(C−O) = 2105.8 cm^{-1}. These values differ by 1.5% and 1.7% from the experimental values of 1.128 Å and 2143 cm^{-1}, respectively,[30] and they are practically identical with the theoretical results reported by Digne et al.[24] Similarly, on the basis of optimizations of an isolated TEDA molecule in a cubic box of length 12 Å, we found that this molecule has D_{3h} symmetry with r(C−C) = 1.5624 Å, r(N−C) = 1.4711 Å, and r(C−H) = 1.0988 Å. These values are very close to those obtained by using Gaussian 03 calculations[14] at the MP2/cc-pVDZ level (r(C−C) = 1.5609 Å, r(N−C) = 1.4723 Å, and r(C−H) = 1.1042 Å).

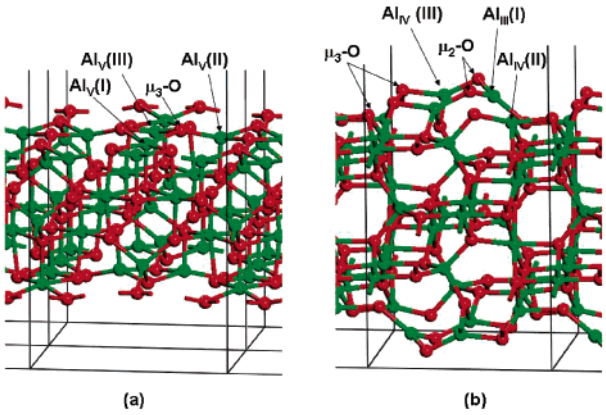

Figure 1. Pictorial view of the slab models used to describe the properties of (a) (100) and (b) (110) surfaces of the γ-Al_2O_3 surface. On the (100) surface the 5-fold coordinated aluminum, Al_V, and 3-fold oxygen, μ-O_3, sites are indicated. On the (110) surface the 3-fold coordinated aluminum, Al_{III}, 4-fold coordinated aluminum, Al_{IV} (II and III), 2-fold coordinated oxygen, μ-O_2, and 3-fold coordinated oxygen, μ-O_3, are indicated.

The agreement between our results for the description of both the bulk and the surfaces of γ-alumina or of isolated TEDA and CO molecules with either experimental values or other high-level first principles calculations gives us confidence for the next step of our investigations, namely, the theoretical investigation of the interactions of TEDA and CO molecules with the (110) and (100) surface of γ-alumina.

III. Results: Experimental Studies

A. CO Adsorption on Nonfunctionalized γ-Al_2O_3, Exposing Brønsted and Lewis Acid Sites. Carbon monoxide adsorption on the γ-Al_2O_3 surface has been studied extensively.[13,31−33] Because of the variety of adsorption sites on the Al_2O_3 surface, several ν(C−O) absorption bands are observed. Figure 2 shows the IR spectrum for CO adsorption onto the Al_2O_3 surface for increasing CO pressure at 130 K. Because of the higher adsorption energy of CO on Lewis acid sites of the Al_2O_3 surface,[31] the absorbance for the vibrational modes at ∼2226 and ∼2185 cm^{-1} develops first and almost saturates at P_{CO} ∼ 2.5 Torr. The adsorbed CO on Al−OH Brønsted acid sites at ν(CO) ≅ 2160 cm^{-1} and the physisorbed CO at ν(CO) ≅ 2143 cm^{-1} begin to form later and continue to develop up to P_{CO} ∼ 15 Torr of CO equilibrium pressure.

B. CO Adsorption on TEDA-Functionalized Al_2O_3. When CO is exposed to a TEDA-precovered Al_2O_3 surface, the CO species observed on the unfunctionalized Al_2O_3 surface are absent and a new feature with ν(CO) ∼ 2135 cm^{-1} is produced as shown in Figure 3. The predosed pressure of the TEDA was chosen in the range of 10−15 mTorr where the binding of TEDA on Al_2O_3 surface was saturated.[1−3] As demonstrated in our previous studies,[1−3] TEDA competes with CO for the Al^{3+}

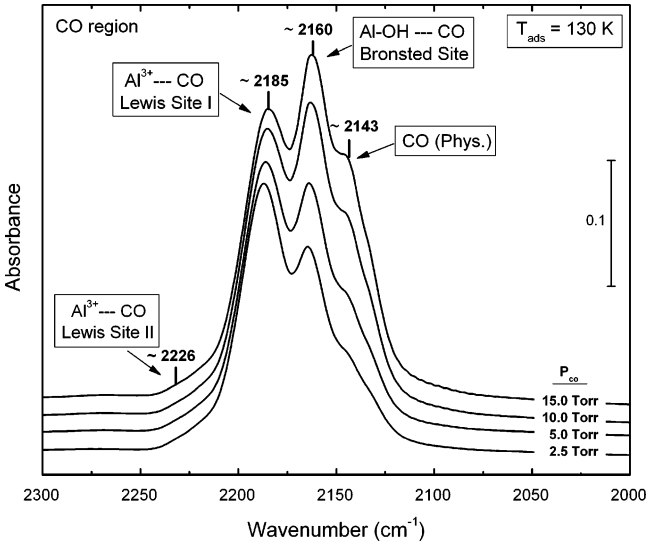

Figure 2. FTIR spectra of the CO adsorption on the Al_2O_3 surface with increasing CO exposure at $P = 2.5$, 5.0, 10.0, and 15.0 Torr and $T = 130$ K.

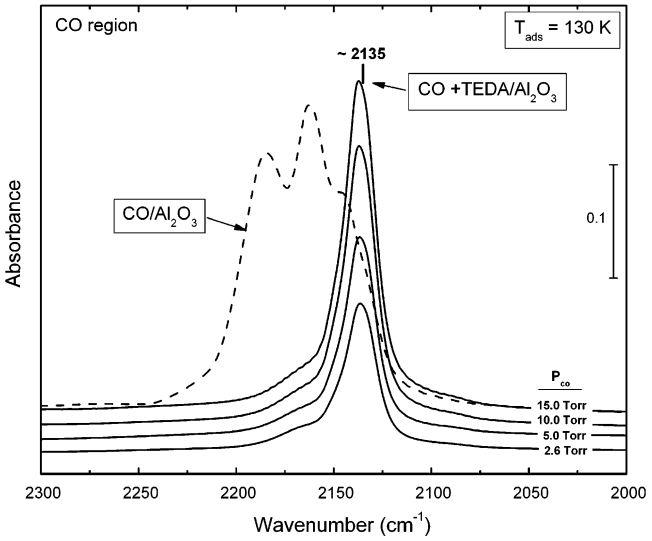

Figure 3. FTIR spectra of the CO adsorption on the TEDA-precovered Al_2O_3 surface with increasing CO exposure at $P = 2.6$, 5.0, 10.0, and 15.0 Torr, compared to the CO adsorption on the unfunctionalized Al_2O_3 surface at 15.0 Torr (dashed line) from Figure 2.

Lewis acid and Al−OH Brønsted acid sites on the Al_2O_3 surface. Since these sites on the surface are already blocked with predosed TEDA, the new feature at ∼2135 cm^{-1} is likely to be caused by the CO and TEDA interaction. However, no significant change in the TEDA vibrational spectral region as well as in the Al−OH region occurs during CO exposure. This reveals that the CO interaction with TEDA is relatively weak.

The dependence of CO binding with the TEDA-functionalized Al_2O_3 as a function of temperature at an equilibrium CO pressure of 15 Torr is shown in Figure 4. The adsorbed CO on the TEDA-precovered Al_2O_3 surface desorbs completely near 200 K. The enthalpy of CO adsorption on the TEDA-precovered surface was measured to be -2.0 ± 0.3 kcal/mol from the van't Hoff plot as shown in the inset of Figure 4. The weakly bound CO adsorbed on TEDA-precovered surfaces exhibits only $\sim 1/3$ the value of ΔH_{ad}(CO) for Lewis acid sites of the Al_2O_3 surface, which is estimated to be in the range of -4.8 to -7.1 kcal/mol.[13,31]

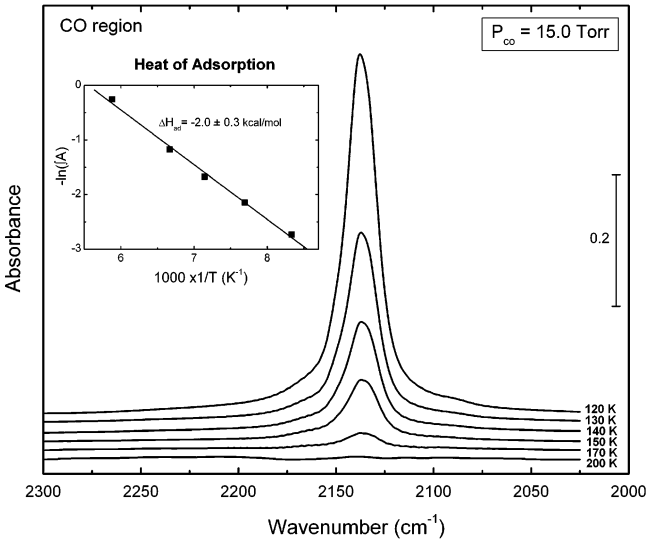

Figure 4. FTIR spectra showing the decrease of CO adsorption on the TEDA-precovered Al_2O_3 surface upon heating to 200 K, while maintaining the equilibrium CO pressure at 15 Torr. The van't Hoff plot of $-\ln(\int A_{CO})$ vs $1/T$ in the left insert yields $\Delta H_{ad}(CO) = -2.0 \pm 0.3$ kcal/mol on TEDA-precovered Al_2O_3.

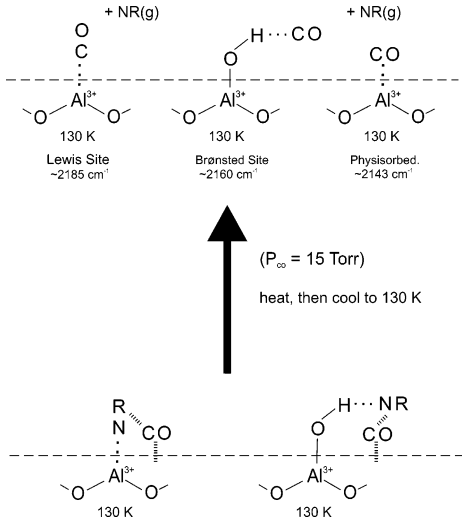

Figure 5. Schematic diagram of the CO adsorption site competition experiment with various amine molecules.

C. Spectroscopic Observation of Site Competition by CO during Amine Desorption from Al_2O_3. Because TEDA[1−3] and other amines desorb intact from Al_2O_3 it is possible to perform a site competition experiment in which the TEDA (or other amine) molecules are slowly removed by thermal desorption in the presence of excess CO(g). As amine desorption occurs, the CO perturbed by the amine disappears and is replaced by CO adsorbed on sites vacated by the amine species. The desorbed amine is condensed on the outer surface of the reentrant Dewar filled with liquid N_2. This experiment is schematically illustrated in Figure 5. At the bottom of Figure 5, a complex of CO with the surface and with the amine (NR) is shown at 130 K. Amine molecules bound to both Al^{3+} sites and to Al−OH groups are indicated, in accordance with our findings for the TEDA molecule.[1−3] As amine molecules desorb thermally to produce NR(g), CO repopulates the surface at sites originally occupied by the amine molecule. Spectroscopic observations are made after cooling to the starting temperature

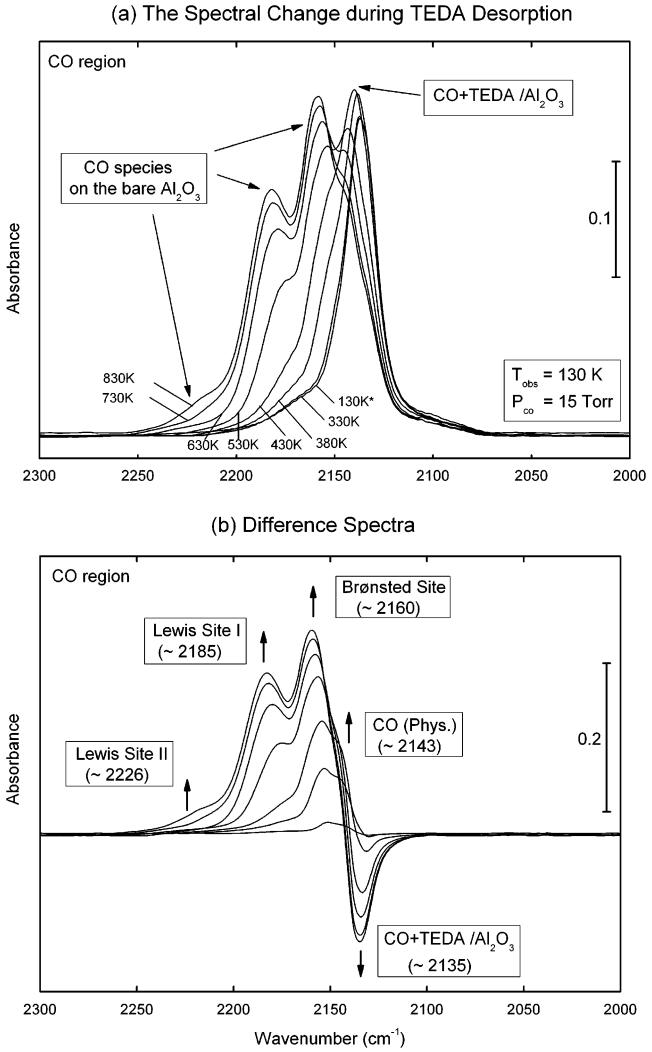

Figure 6. The spectral change of the adsorbed CO on the TEDA-precovered Al_2O_3 surface (a) before (130 K) and after heating the sample to $T = 330$, 380, 430, 530, 630, 730, and 830 K. All the spectra were taken at 130 K, at an equilibrium CO pressure of 15.0 Torr. (b) The difference spectra obtained by subtracting the original spectrum which is noted as 130 K in part a.

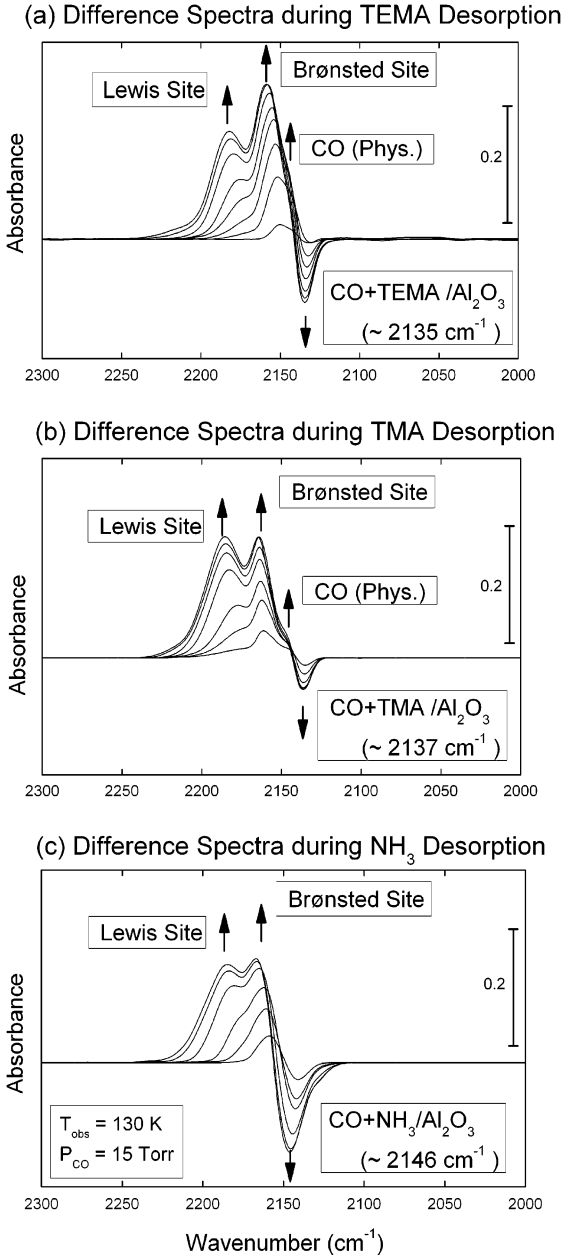

Figure 7. The difference spectra of adsorbed CO on (a) the TEMA-precovered Al_2O_3 surface before and after heating the sample to $T = 330$, 380, 430, 480, 530, 630, 730, and 830 K, (b) the TMA-precovered Al_2O_3 surface before and upon heating the sample to $T = 330$, 380, 430, 530, 630, 730, and 830 K, and (c) the NH_3-precovered Al_2O_3 surface before and upon heating the sample to $T = 330$, 380, 430, 480, 530, 630, and 730 K. All the spectra were taken at 130 K after heating, at an equilibrium CO pressure of 15.0 Torr.

of 130 K following desorption experiments at successively higher temperatures.

Figure 6 shows a sequence of experiments supporting the scheme in Figure 5 in which heating up to 830 K is carried out, followed by cooling under excess CO(g). Figure 6a shows the actual spectra; Figure 6b shows difference spectra which are very informative. In Figure 6b we observe the loss of the CO absorbance at ~2135 cm^{-1} associated with the CO···TEDA/Al_2O_3 complex, and the concomitant formation of CO species bound to Brønsted sites and to the two types of Lewis acid sites. In addition, evidence for CO physisorption (~2143 cm^{-1}) is seen clearly in the difference spectra.

Figure 7 shows a set of difference spectra for similar experiments to those of Figure 6, in which TEMA, TMA, and NH_3 adsorbates are systematically desorbed with site repopulation by CO. The temperature range for each experiment is given in the figure caption. TEDA, TEMA, TMA, and ammonia functionalities behave very similarly in the following ways: (1) a complex between the CO and the various amines is observed in each case with a low ν(CO) frequency (compared to CO(g)) and (2) this complex disappears as heating under CO(g) takes place and both Al−OH···CO and Al^{3+}−CO species are recovered as the amine coverage decreases, vacating Al−OH and Al^{3+} sites.

D. Comparative Studies of Amine Desorption by FTIR. Figure 8 shows a plot of the normalized amine desorption behavior for the four molecules which form a surface complex with adsorbed CO, causing its C−O frequency to decrease. The normalized absorbances of the δ(N−H) mode at ~1240 cm^{-1} (NH_3) and the δ(C−H) modes at ~1240 (TMA), ~1202 (TEMA), and ~1323 cm^{-1} (TEDA) are plotted as a function of the temperature as shown in Figure 8. To within our experimental error, all four amines exhibit similar behavior in their desorption kinetics. This behavior is a composite of amine desorption processes from both Al−OH bonding sites and Al^{3+}

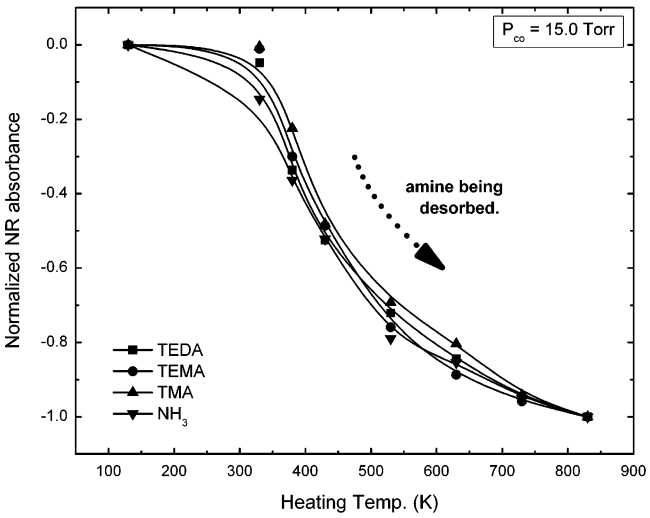

Figure 8. The decrease in the normalized absorbance of a selected vibrational mode of the precovered amine upon heating in steps to 830 K in the CO adsorption site competition experiment. The δ(N−H) mode at ∼1240 cm^{-1} (NH_3) and the δ(C−H) modes at ∼1240 (TMA), ∼1202 (TEMA), and ∼1323 cm^{-1} (TEDA) are selected in each measurement.

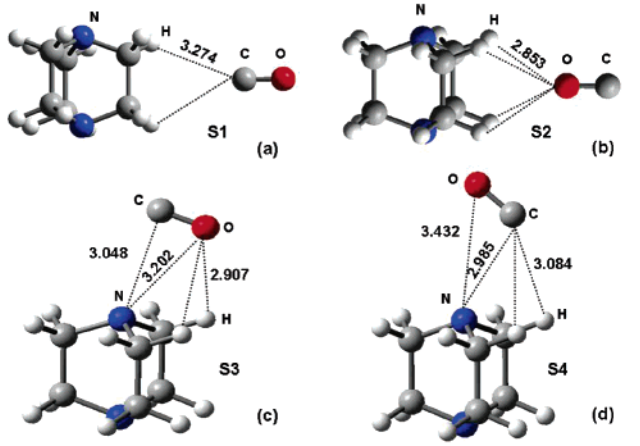

Figure 9. Pictorial view of the isomeric forms of the TEDA−CO complex as determined based on molecular orbital calculations at the MP2/cc-pVDZ level of theory: (a) edge perpendicular structure (S1), (b) face perpendicular structure (S2), and (c and d) end-tilt structures (S3 and S4).

bonding sites, and desorption occurs over a very wide temperature range by a sequence of kinetic processes which are not investigated in this work.

IV. Results: Theoretical Studies

A. Interaction of CO and TEDA Molecules in the Gas Phase. In a first set of theoretical investigations we focused on a description of the interaction properties between CO and TEDA molecules in the gas phase. Several configurations of the CO molecule around TEDA have been considered corresponding to face, bridge, and end-on conformations. In each case, frequency calculations have been performed to confirm the existence of a local minimum on the potential energy surface. The resulting configurations, which have been found to correspond to a local minimum on the potential energy surface, are presented in Figure 9. In this figure, the edge and face perpendicular structures S1 and S2 have been found to have C_{2v} symmetry while the end tilted configurations S3 and S4 have C_s symmetry. In all four cases the CO bond distances seem to be little affected with values ranging between 1.147 and 1.148 Å. Similarly, the CO stretching frequencies are only weakly modified relative to the MP2/cc-pVDZ calculated vibrational frequency of isolated CO of 2113.9 cm^{-1}, namely $\Delta\nu_1 = 1.0$ cm^{-1} for S1, $\Delta\nu_2 = -8.9$ cm^{-1} for S2, $\Delta\nu_3 = -9.9$ cm^{-1} for S3, and $\Delta\nu_4 = -2.9$ cm^{-1} for S4. When the above identified structures are further optimized by considering the counterpoise correction, we found that only structures S2 and S4 correspond to a local minimum. The S1 structure was found to correspond to a second-order saddle point while structure S3 is a transition state. Using the basis set superposition error corrected energies we estimate very small binding energies of CO to TEDA with values of 0.48 kcal/mol for S2 and 1.1 kcal/mol for S4 configurations, respectively. These results indicate very small interaction energies between TEDA and CO molecules in the gas phase.

B. Adsorption and Coadsorption of CO and TEDA Molecules on (100) and (110) Surfaces of γ-Al_2O_3. The adsorption studies of individual CO and TEDA molecules and the coadsorption of TEDA−CO molecules on the γ-Al_2O_3 surface were done by using the slab models presented in Figure 1, corresponding to the (100) and (110) surface orientations. The corresponding adsorption energies calculated throughout this work were obtained based on the expression

$$E_{ads} = E_{molec} + E_{slab} - E_{(molec+slab)} \quad (1)$$

where E_{molec} is the energy of the isolated adsorbate molecule in its equilibrium position, E_{slab} is the total energy of the slab, and $E_{(molec+slab)}$ is the total energy of the adsorbate/slab system. A positive E_{ads} corresponds to a stable adsorbate/slab system. The energy of the isolated adsorbate molecule was determined from calculations performed on a single molecule in a cubic cell of length 12 Å. The same Brillouin-zone sampling has been used to calculate the energies of the bare slab and of the molecule−slab systems.

As the current experimental work has been done in high vacuum conditions with surfaces annealed up to 1000 K it is considered that the main spectral features observed will be mainly due to interaction of adsorbates with unsaturated Al ion sites. Consequently, in our theoretical work we have focused first on the description of adsorption at these sites and on identification of the corresponding CO stretching frequencies. The corresponding results related to adsorption of isolated CO molecules on (100) and (110) surfaces of γ-Al_2O_3 surface are presented in Table 1 while representative configurations are depicted in Figure 10a−c. We found that on the (100) surface, the CO molecule binds on Lewis Al^{3+} sites with adsorption energies ranging from 4.6 to 9.5 kcal/mol while on the (110) surface the binding increases to values up to 17.1 kcal/mol. The higher binding energies correspond to Al atoms with a high degree of unsaturation as is the case of Al_{III}(I) sites on the (110) surface. Corresponding to these changes in the binding energy there is also a corresponding upward vibrational shift (blueshift) in the range of 10−64 cm^{-1} (see section a in Table 1) with the largest shifts obtained for the case of the (110) surface. These results are very similar to those reported before by Digne et al.,[24] who have analyzed in detail the effect of hydration upon the surface Lewis acidity.

In the case of TEDA adsorption, the results of adsorption calculations are also given in section b of Table 1 while representative configurations are depicted in Figure 10, panels d−f. It can be seen from these figures and data in Table 1 that the TEDA molecule adsorbs with N toward the unsaturated Al sites of the surface at Al···N separations in the range 2.014−2.323 Å. Similar to the CO case, adsorption of the TEDA

TABLE 1: Calculated Equilibrium Distances and Adsorption Energies for CO, TEDA, and OH Molecules on (100) and (110) Surfaces of γ-Al_2O_3[a,b]

system/surface	site	d(Al···CO)/[c] d(Al···OH)	d(C−O)/ [c]d(O−H)	d(Al···N)/ d(OH···N)	E_{ads}[d]	$\delta\nu$(C−O)
(a) CO adsorption						
(100)	Al_V(I)	2.158	1.141		9.5	24.2
	Al_V(II)	2.305	1.142		4.6	16.2
	Al_V(III)	2.231	1.142		5.3	10.1
(110)	Al_{III}(I)	2.136	1.137		17.1	64.1
	Al_{IV}(II)	2.184	1.141		9.6	28.2
	Al_{IV}(III)	2.239	1.142		4.0	21.4
(b) TEDA adsorption						
(100)	Al_V(I)			2.244	19.3	
	Al_V(II)			2.323	13.8	
	Al_V(III)			2.152	18.3	
(110)	Al_{III}(I)			2.014	40.0	
	Al_{IV}(II)			2.080	27.0	
	Al_{IV}(III)			2.145	17.4	
(c) CO···TEDA coadsorption						
(100)	T(Al_V(I))−CO(Al_V(II))	2.256	1.147	2.265	4.6	−26.1
	T(Alv(I))−CO(Alv(III))	2.632	1.146	2.251	0.4	−17.8
	T(Al_V(III))−CO(Al_V(I))	2.232	1.145	2.237	1.1	−18.8
	T(Alv(III))−CO(Alv(II))	2.355	1.145	2.168	1.8	−17.0
(110)	T(Al_{III}(I))−CO(Al_{IV}(III))	2.457	1.141	2.013	2.8	−10.6
	T(Al_{IV}(II))−CO(Al_{IV}(III))	2.372	1.148	2.093	1.0	−29.1
(d) OH Adsorption						
(100)	μ_1-Al_V(I)	1.809	0.974		37.5	
	μ_1-Al_V(II)	1.858	0.977		28.6	
	μ_1-Al_V(III)	1.771	0.970		35.0	
(110)	μ_1-Al_{III}(I)	1.692	0.968		61.1	
	μ_1-Al_{IV}(III)	1.792	0.974		35.7	
	μ_2-Al_{IV}(III)	1.936	0.975		44.7	
(e) OH−TEDA adsorption						
(100)	μ_1-Al_V(III)−TEDA	1.791	0.973	2.171	16.4	
(110)	μ_1-Al_{III}(I)−TEDA	1.697	0.975	1.977	17.9	
	μ_1-Al_{IV}(II)−TEDA	1.773	0.981	2.102	18.3	
	μ_2-Al_{IV}(II)−TEDA	1.954	0.983	2.214	17.0	
f) OH−TEDA···CO coadsorption						
(100)	OH(Alv(III))−TEDA...	1.780	0.977	2.068		
	CO(Al_V(II))	2.229	1.147		6.4	−26.0
(110)	μ_1-Al_{III}(II)−TEDA...	1.710	0.974	2.067		
	CO(Al_{IV}(III))	2.488	1.150		2.4	−51.0
	μ_1-Al_{III}(II)−TEDA...	1.778	0.980	2.129		
	CO(Al_{IV}(II))	2.216	1.144		5.0	−11.8

[a] In the case of CO structures the corresponding frequency shift $\delta\nu$(C−O) with respect to the calculated gas phase vibration frequency of 2105.8 cm^{-1} is also indicated. [b] Bond distances are given in Angstroms, adsorption energies in kcal/mol, and vibrational frequency shifts in cm^{-1}. [c] The bond distance d(Al...CO) is considered in the case of CO adsorption, d(Al...OH) is considered in the case of OH adsorption and d(OH...N) is considered for TEDA binding to OH group. Similarly, d(C−O) and d(O−H) relate the corresponding bond distances in the case of CO and respectively, OH adsorption. [d] In the case of coadsorption studies only the adsorption energy of CO is reported; this was calculated with respect to isolated gas-phase CO molecule and the surface with preadsorbed TEDA or OH-TEDA molecules, respectively.

molecule is the strongest in the case of the (110) surface, particularly for the case of binding at Al_{IV}(II) and Al_{III}(I) sites which are the most uncoordinated. In these cases the binding energy increases to 27 and 40 kcal/mol, respectively. On the basis of these results it follows that the TEDA molecule interacts significantly more strongly with both (100) and (110) surfaces of γ-Al_2O_3 compared to CO.

One main implication of the above presented results is that in the case of coadsorption studies in which the TEDA molecule was adsorbed prior to CO adsorption, it is expected that all surface sites which present the strongest interaction with TEDA, namely Al_V(I) on the (100) surface and respectively Al_{III}(I) and Al_{IV}(II) sites on the (110) surface, will be primarily occupied by TEDA molecules. To further understand the effect upon binding and vibrational properties of CO when exposed to a TEDA-precovered Al_2O_3 surface we have considered that the TEDA molecule will occupy the most stable surface sites while the CO molecule will adsorb at nearby surface sites, exhibiting an interaction with TEDA. The corresponding results are given in section c of Table 1 while representative configurations are depicted in Figure 11. From the data given in Table 1 it follows that a significant weakening of the CO bonding to the surface takes place in the vicinity of a bound TEDA molecule. In particular, in the case of the (110) surface which is the dominant orientation in the case of polycrystalline Al_2O_3, the binding energies of CO on the TEDA-precovered surface have small values in the range 1.0−2.8 kcal/mol. This binding energy compares favorably with the experimental result (2.0 ±0.3 kcal/mol) shown in Figure 4. Our calculations also show that for both (100) and (110) surface orientations, important downward shifts of the C−O vibrational frequencies occur compared to gas-phase CO with shifts in the range −10.6 to −29.1 cm^{-1}. The experimental shift for the CO···TEDA/Al_2O_3 case is −8 cm^{-1} as seen in Figure 5.

Besides adsorption at the unsaturated Al^{3+} sites, we have also analyzed the possibility of TEDA molecules adsorbing at Al−OH Brønsted acid sites. In their previous study Digne et al.[24] have done a systematic study of the hydration process for

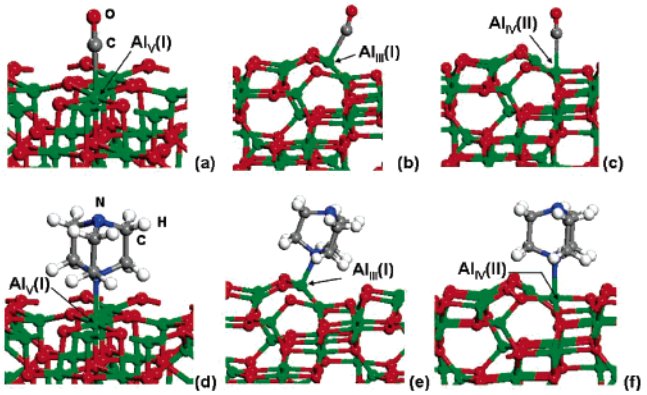

Figure 10. Representative adsorption configurations of CO and TEDA molecules on (100) and (110) γ-Al_2O_3 surfaces. Panels a and d correspond to the (100) surface while the remaining panels correspond to the adsorption configuration on the (110) surface.

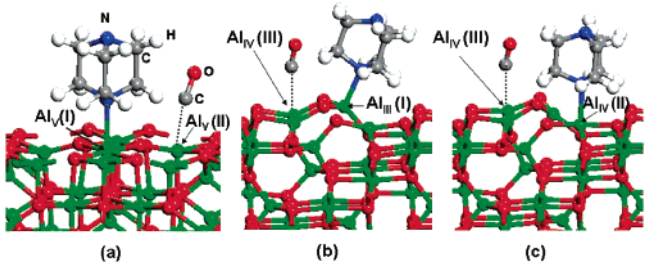

Figure 11. Representative coadsorption configurations of TEDA and CO molecules on (100) Al_2O_3 (panel a) and (110) Al_2O_3 (panels b and c).

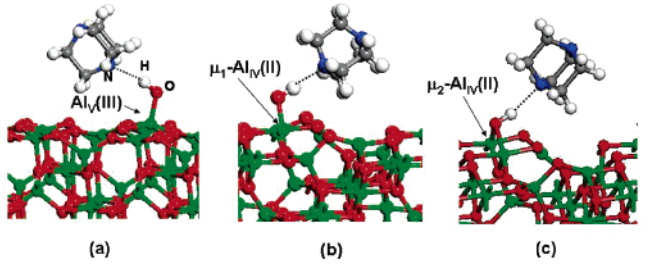

Figure 12. Representative adsorption configurations of TEDA molecule at OH Brønsted sites on (100) Al_2O_3 (panel a) and (110) Al_2O_3 (panels b and c).

γ-alumina and of the corresponding modifications of OH-stretching frequencies. In this study we will restrict our investigations to the case of small coverage of OH species with the intention to determine how the TEDA molecule will adsorb at such sites. The corresponding results are presented in sections d and e of Table 1. Our calculations confirm that the TEDA molecule adsorbs on hydroxyl groups by formation of O−H···N hydrogen bonds. This confirms earlier experimental studies.[3] As indicated in Table 1 the OH···N bond distances exhibit variations between 2.095 and 2.214 Å. The highest binding energy of 31.9 kcal/mol is obtained for the case when the OH group is adsorbed at the $Al_{III}(I)$ unsaturated site on the (110) surface. However, in all the other cases we investigated there is only a small dependence on the surface site and OH orientation, as reflected by the corresponding binding energies with values in the range 16.4−18.3 kcal/mol for the OH···TEDA binding energy, in the limit of zero coverage. Experiments[3] measured an energy of ∼3.7 kcal/mol, which is probably so low compared to the calculated energy because of the higher TEDA coverage in the experiments.

A final point we have analyzed was related to modifications of the CO vibrational frequencies in the case of coadsorption with TEDA molecules adsorbed at hydroxyl sites. This point has been considered only for a few configurations indicated in Table 1, section f. The results obtained indicate a downward shift of CO vibrational frequencies relative to gas-phase values. Consequently, our calculations support the fact that independent of the type of Lewis or Brønsted surface sites at which the TEDA molecule adsorbs on the surface, when CO molecules are coadsorbed at nearby unsaturated aluminum sites a downward shift of the CO vibrational mode frequency will take place.

V. Discussion

A. CO Adsorption on the TEDA-Precovered Al_2O_3 Surface. In this study we found a weakly bound CO species on the TEDA-precovered Al_2O_3 surface. The existence of this CO··· TEDA complex species with ν(CO) ∼ 2135 cm^{-1} is evident from the TEDA thermal desorption experiment (Figure 6). As the coverage of TEDA is decreased by successive heating, the absorbance of adsorbed CO species on the TEDA-precovered surface also decreases in the difference spectrum as shown Figure 6b. By heating the sample to 830 K most of the TEDA (∼99%) desorbs from the surface. As a result, the spectral feature in the CO region (see Figure 6a) becomes identical with that observed in Figure 2, corresponding to CO adsorption on the unfunctionalized Al_2O_3 surface.

Additional insight into the geometry of the CO···TEDA complex can be obtained by analyzing CO adsorption on TEMA-precovered surfaces. TEMA has the same cage structure as TEDA with one of the terminal nitrogen atoms replaced by a carbon atom. The spectrum of the adsorbed TEMA on Al_2O_3 surfaces (not shown here) shows the production of a broad band centered at ∼3530 cm^{-1}, which is assigned to the Al−OH mode that has been shifted due to interaction with the TEMA molecule, while the δ(C−N) mode is redshifted by −8 cm^{-1} from the gas-phase frequency. These vibrational spectral changes agree with the idea that TEMA also adsorbs on the Al_2O_3 surface via the N atom anchored to surface as would be expected. Upon TEMA adsorption followed by exposure to CO(g) a new spectral feature at 2135 cm^{-1} is observed (see Figure 7a), similar to that observed in the case of CO adsorption on the TEDA-functionalized surface. This result indicates that it would be very unlikely that a CO molecule binds to the exposed N atom of TEDA molecules in an end-on bonding configuration, since ν(CO) for the TEDA···CO and the TEMA···CO complexes are identical. These findings are also consistent with the results of ab initio molecular orbital calculations. As is discussed in Section IV.A, the interactions between TEDA and CO molecules in the gas phase are very weak, with binding energies in the range 0.5−1.0 kcal/mol. For this reason it is expected that direct bonding of CO and TEDA molecules is not significant and consequently on the Al_2O_3 surface the CO molecule will rather bind to the surface sites unoccupied by TEDA molecules, and will be weakly influenced by neighbor TEDA molecules. In our experimental work, adsorption of CO was carried out on a TEDA-precovered surface. It is expected that TEDA molecules will occupy the most energetically favorable sites while CO molecules will be positioned on the remaining surface sites in the vicinity of TEDA molecules. On the basis of this surface occupation scheme, our calculated results presented in section c of Table 1 have shown that a significant weakening of CO binding with the surface takes place in the case of TEDA−CO coadsorption relative to the case when only CO molecules are adsorbed on the surface. Consistent with this binding energy

TABLE 2: The Effect of Amine Derivatives on the Frequency Shifts of Adsorbed CO

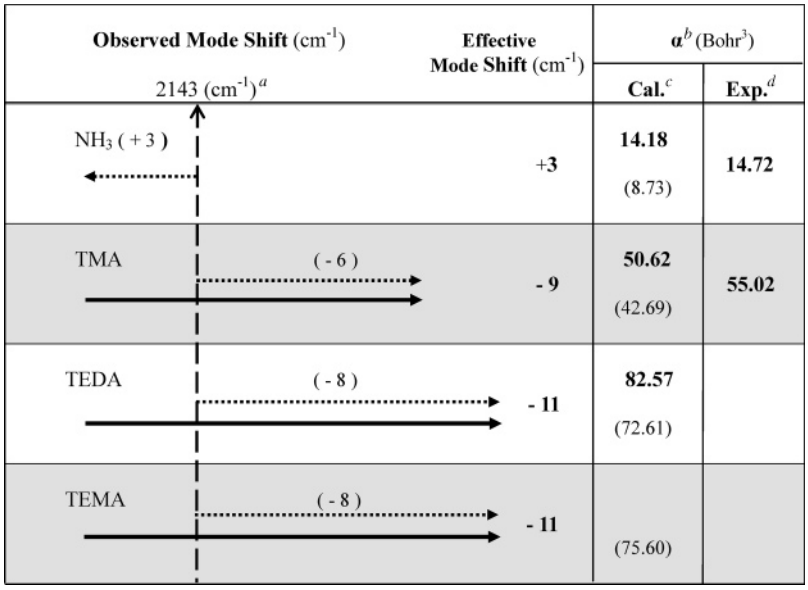

[a] The frequency of the CO vibrational mode in the gas phase. [b] Isotropic polarizability. [c] The calculation was done at the MP2/aug-cc-pVTZ level with the Gaussian 03 program. The values in parentheses are from the calculation with the MP2/cc-pVDZ basis set. [d] The experimental values are from ref 40.

trend, we have determined that the CO modes in the TEDA···CO complex are redshifted by −10.6 to −29.1 cm^{-1} compared to the vibrational frequency of CO in the gas phase. These theoretical findings are also in agreement with our experimental results where a ν(CO) redshift of −8 cm^{-1} is observed.

B. CO Adsorption on the Clean Al_2O_3 Surfaces. In this work the Al_2O_3 sample was prepared by heating at 1000 K and the oxide surface is mostly dehydrated and exposes mainly unsaturated Al^{3+} sites. We have shown in the theoretical section (see Figure 1) that several Al_V, Al_{IV}, and Al_{III} unsaturated aluminum atom sites (Lewis acid sites) can be identified on both (100) and (110) surfaces with the (110) surface having a higher surface density of broken Al−O bonds[24] than the (100) surface. The results of our DFT plane-wave calculations in conjunction with slab model calculation have indicated that both TEDA and CO molecules can adsorb at these unsaturated Al ion sites, but the bonding energy of TEDA molecules is higher than that of CO molecules on these sites. Upon adsorption at such Lewis acid sites, a blueshift in ν(CO) in the range of 10 to 64 cm^{-1} relative to the gas-phase value has been determined for ν(CO). Such a blueshift is caused by strong electron-withdrawing properties of the Al^{3+} sites. This shift is correlated to the strength of CO bonding to the surface, which varies in the order $E_{ads}(Al_V) \leq E_{ads}(Al_{IV}) < E_{ads}(Al_{III})$. It is highest in the case of Al_{III} sites on the (110) surface.

C. TEDA Adsorption on the Clean Al_2O_3 Surface. Besides adsorption of TEDA on unsaturated Al sites we have determined that TEDA molecules can also adsorb on Brønsted OH sites by formation of OH···N hydrogen bonds.[2,3] As determined by theory, the binding in this case occurs with energies in the range 16.4−18.3 kcal/mol, which is somewhat weaker than found for direct TEDA bonding to unsaturated Al sites. Additionally, on the basis of a limited set of coadsorption studies, we have determined that the CO vibrational frequency for the OH··· TEDA···CO complex is also redshifted relative to the gas-phase value. These results suggest that the measured shift of the CO vibrational frequency can be used both as a measure of the surface acidity as well as an indicator of the amount of TEDA (or other amine molecules) present on the surface.

D. Perturbation of Adsorbed CO on Various Amine-Precovered Surfaces. In the site competition experiment with TMA and NH_3, as the precovered amine desorbs thermally, the difference spectra in the CO vibrational mode region also indicate the loss of a weakly interacting CO···TEDA complex, as is shown in Figure 7b,c. In the report by Hadjiivanov et al.[34] they could not find any evidence of a direct interaction between CO and preadsorbed NH_3 on a TiO_2 surface. They mentioned the possibility that CO might adsorb physically on the ammonia-covered part of the surface judging by the enhancement of the physically adsorbed CO mode after coadsorption. In our current work, the shifted ν(CO) mode of the weak CO···amine complex was clearly resolved by the site competition experiment.

The observed mode shifts of CO on various amine-precovered surfaces are shown in Table 2 together with the polarizability value for each amine as determined from ab initio molecular orbital calculations. It can be observed that as the CO molecule interacts with polarizable amine molecules in the order NH_3 < TMA < TEMA/TEDA, the ν(CO) vibrational frequency of the CO···amine complex appears to move increasingly downward, as the amine polarizability increases, as would be expected for vibrational shifts due primarily to image effects.[35]

The desorption behavior of amines on Al_2O_3 is monitored by plotting the normalized absorbance of the vibrational mode of the various amines upon desorption, as shown Figure 8. The essentially coincident curves for the four amines show that there is little difference in the desorption kinetics of these amines on Al_2O_3 surfaces. The amount of remaining amine after heating to 830 K can be estimated by integrating the absorbance of one of the selected vibrational modes. The final coverage of amines is below ∼5% of the initial amount of amine on the surface in all cases. All the amines which are used in this study are classified as strong bases by the value of the ionization constants of onium acids ($pK_a(BH^+)$) which are in the range of 8.5 to 11.0. On the assumption that these amines have similar reactivity and binding to the Al_2O_3 surface, the trend of showing more downward CO vibrational frequency shift with the more polarizable amine molecule can be explained best by the image dipole effect for the dynamic dipole of the CO molecule. As the polarizability of a preadsorbed amine become larger, the

amine would support a stronger induced image dipole for the CO oscillator, resulting in stronger damping and in a larger redshift.[35−39] Since the chemical bonding effect between CO and chemisorbed amine can be estimated to be $+3$ cm^{-1} from the mode shift of CO on the ammonia-precovered surface (where there is little image-dipole effect for the NH_3), the real dynamic dipole image effects of other amines can be deduced as shown in Table 2, using the $+3$ cm^{-1} shifted frequency as a reference.

VI. Summary

The interaction of CO and triethylenediamine (TEDA) coadsorbed on γ-Al_2O_3, has been studied with transmission infrared spectroscopy and first principles theory. The following results have been obtained:

1. The interaction of the adsorbed TEDA molecule with chemisorbed CO on γ-Al_2O_3 is very weak as indicated by the presence of a slightly redshifted ν(CO) mode at $\sim$2135 cm^{-1}. The studies with CO will therefore provide a comparison to other molecule−amine surface complexes where strong interactions are expected.

2. The enthalpy of CO adsorption on the TEDA-functionalized surface is measured to be -2.0 ± 0.3 kcal/mol, which is much smaller than the enthalpy of CO adsorption on the unfunctionalized surface (-4.8 to -7.1 kcal/mol).

3. By comparing the interaction of CO with TEDA-functionalized and TEMA-functionalized surfaces, no evidence is found for the bond formation between CO and the exposed basic N atom of the TEDA functionality.

4. First principles theoretical analysis indicates that chemical bond formation between adsorbed TEDA and CO is absent and that the observed decrease in CO binding energy for a TEDA-functionalized surface is expected.

5. The small redshift in ν(CO), due to interaction with a series of coadsorbed amines on Al_2O_3, increases as the polarizability of the amine increases, indicating that image dipole effects are mainly involved in causing damping of the CO oscillator.

Acknowledgment. We acknowledge with thanks the support of this work by The Army Research Office, and discussion with Dr. Alex Balboa of Aberdeen Proving Ground and with Dr. Joseph Rossin of Guild Associates. Grants of computer time at the Army Research Laboratory and Pittsburgh Supercomputer Center are also gratefully acknowledged.

References and Notes

(1) Kim, S.; Byl, O.; Yates, J. T., Jr. *J. Phys. Chem. B* **2005**, *109*, 6331.
(2) Kim, S.; Byl, O.; Yates, J. T., Jr. *J. Phys. Chem. B* **2005**, *109*, 3499.
(3) Kim, S.; Byl, O.; Yates, J. T., Jr. *J. Phys. Chem. B* **2005**, *109*, 3507.
(4) Wren, J. C.; Long, W.; Moore, C. J.; Weaver, K. R. *Nucl. Technol.* **1999**, *125*, 13.
(5) Rossin, J. A.; Morrison, R. W. *Carbon* **1991**, *29*, 887.
(6) Pickett, J. L.; Naderi, M.; Chinn, M. J.; Brown, D. R. *Sep. Sci. Technol.* **2002**, *37*, 1079.
(7) Iu, K.-K.; Thomas, J. K. *J. Photochem. Photobiol., A: Chem.* **1993**, *71*, 55.
(8) Hall, C. R.; Sing, K. S. *Chem. Br.* **1988**, *24*, 670.
(9) Peri, J. B.; Hannan, R. B. *J. Phys. Chem.* **1960**, *64*, 1526.
(10) Knözinger, H.; Ratnasamy, P. *Catal. Rev. Sci. Eng.* **1978**, *17*, 31.
(11) Cornelius, E. B.; Miliken, T. H.; Mills, G. A.; Oblad, A. G. *J. Phys. Chem.* **1955**, *59*, 809.
(12) Ballinger, T. H.; Wong, J. C. S.; Yates, J. T., Jr. *Langmuir* **1992**, *8*, 1676.
(13) Ballinger, T. H.; Yates, J. T., Jr. *Langmuir* **1991**, *7*, 3041.
(14) Frisch, M. J.; et al. *Gaussian 03*, Revision C.02; Gaussian, Inc.: Wallingford CT, 2004.
(15) Kresse, G.; Hafner, J. *Phys. Rev.* **1993**, *B 48*, 13115.
(16) Kresse, G.; Furthmüller, J. *Comput. Mater. Sci.* **1996**, *6*, 15.
(17) Kresse, G.; Furthmüller, J. *Phys. Rev.* **1996**, *B 54*, 11169.
(18) Vanderbilt, D. *Phys. Rev.* **1990**, *B 41*, 7892.
(19) Kresse, G.; Hafner, J. *J. Phys. Condens. Matter* **1994**, *6*, 8245.
(20) See VASP manual at http://cms.mpi.univie.ac.at/vasp/vasp/vasp.html.
(21) Perdew, J. P.; Chevary, J. A.; Vosko, S. H.; Jackson, K. A.; Pedersen, M. R.; Singh, D. J.; Fiolhais, C. *Phys. Rev.* **1992**, *B 46*, 6671.
(22) Monkhorst, H. J.; Pack, J. D. *Phys. Rev.* **1976**, *B 13*, 5188.
(23) Kresse, G.; Hafner, J. *Phys. Rev.* **1993**, *B 47*, 588.
(24) Digne, M.; Sautet, P.; Raybaud, P.; Euzen, P.; Toulhoat, H. *J. Catal.* **2004**, *226*, 54.
(25) Murnaghan, F. D. *Proc. Natl. Acad. Sci. U.S.A.* **1944**, *30*, 244.
(26) Wilson, S. J. *J. Solid. State Chem.* **1979**, *30*, 247.
(27) Ealet, B.; Elyakhlouffi, M. H.; Gillet, E.; Ricci, M. *Thin Solid Films* **1994**, *250*, 92.
(28) Beaufils, J. P.; Barbaux, Y. *J. Chim. Phys.* **1981**, *78*, 347.
(29) Nortier, P.; Fourre, P.; Mohammed Saad, A. B.; Saur, O.; Lavalley, J. C. *Appl. Catal.* **1990**, *61*, 141.
(30) Huber, K. P.; Herzberg, G. *Molecular Spectra and Molecular Structure*; Constants of Diatomic Molecules, Vol. VI; Van Nonstrand: New York, 1979.
(31) Zecchina, A.; Platero, E. E.; Areán, C. O. *J. Catal.* **1987**, *107*, 244.
(32) Zaki, M. I.; Knözinger, H. *Mater. Chem. Phys.* **1987**, *17*, 201.
(33) Zaki, M. I.; Knözinger, H. *Spectrochim. Acta* **1987**, *43A*, 1455.
(34) Hadjiivanov, K.; Lamotte, J.; Lavalley, J.-C. *Langmuir* **1997**, *13*, 3374.
(35) Hallam, H. E., Ed. *Vibrational Spectroscopy of Trapped Species*; Wiley: London, UK, 1973.
(36) Buckingham, A. D. *Proc. R. Soc. London* **1958**, *A248*, 169.
(37) Antoniewicz, P. R.; Cavanagh, R. R.; Yates, J. T., Jr. *J. Chem. Phys.* **1980**, *73*, 3456.
(38) Tipler, P. A. *Physics*, 2nd ed.; Worth Publishers: New York, 1982.
(39) Beebe, T. P.; Gelin, P.; Yates, J. T., Jr. *Surf. Sci.* **1984**, *148*, 526.
(40) Lide, D. R.; et al. *Handbook of Chemistry and Physics*, 84th ed.; CRC Press: Boca Raton, FL, 2003.